# miR-494 inhibits cell proliferation and metastasis via targeting of CDK6 in osteosarcoma

WEI YUAN[1], DU WANG[2], YANG LIU[1], DONGDONG TIAN[1], YANG WANG[1], RANXI ZHANG[1], LIANGJUN YIN[1] and ZHONGLIANG DENG[1,3]

[1]Department of Orthopedic Surgery, The Second Affiliated Hospital, Chongqing Medical University, Chongqing 400010; [2]Department of Orthopedics, Wuhan Hospital No. 3 and Tongren Hospital of Wuhan University, Wuhan, Hubei 430060; [3]Chongqing Clinical Research Center in Geriatrics, Chongqing 400010, P.R. China

Received October 10, 2016; Accepted June 1, 2017

DOI: 10.3892/mmr.2017.7709

**Abstract.** Tumorigenesis is a multistep process involving various cell growth-associated factors. Accumulated evidence indicates that the disordered regulation of microRNAs (miRNAs) contributes to tumorigenesis. However, the detailed mechanism underlying the involvement of miRNAs in oncogenesis remains to be fully elucidated. In the present study, the repressed expression of microRNA (miR)-494 was identified in 18 patients with osteosarcoma (OS) and OS cell lines, compared with corresponding controls. To determine whether deregulated miR-494 exerts tumor-suppressive effects in the development of OS, the effects of miR-494 on cell proliferation and metastasis were evaluated. It was found that the restoration of miR-494 in MG-63 and U2OS cells led to inhibited cell proliferation and attenuated migratory propensity *in vitro*, determined through analysis using MTT, colony formation and Transwell assays. In addition, overexpression of miR-494 markedly suppressed the tumor volume and weight *in vivo*. In accordance, the ectopic expression of miR-494 induced cell cycle arrest at the G1/S phase in OS cells. Bioinformatics analysis and luciferase reporter assays were performed to investigate the potential regulatory role of miR-494, the results of which indicated that miR-494 directly targeted cyclin-dependent kinase 6 (CDK6). Of note, the data obtained through reverse transcription-quantitative polymerase chain reaction and western blot analyses suggested that the elevated expression of miR-494 resulted in reduced mRNA and protein expression levels of CDK6. Taken together, these findings indicated that the miR-494/CDK6 axis has a significant tumor-suppressive effect on OS, and maybe a diagnostic and therapeutic target for the treatment of OS.

*Correspondence to:* Dr Zhongliang Deng, Department of Orthopedic Surgery, The Second Affiliated Hospital, Chongqing Medical University, 76 Linjiang Road, Chongqing 400010, P.R. China
E-mail: zhongliang.deng@qq.com; zhongld97@163.com

*Key words:* cyclin-dependent kinase 6, osteosarcoma, proliferation, metastasis, microRNA-494

## Introduction

Osteosarcoma (OS) is a mesenchymal tumor, which is a primary aggressive type of bone cancer typically presenting in children and young adults. The causes of OS can be summarized as a complex of genetic, epigenetic and biological factors. Although there have been advances in treatment, the clinical outcomes for patients with OS have not improved substantially and the survival rate of patients remains at only ~15-30% (1-3). Therefore, the development of more effective diagnostic and treatment methods for OS is urgently required.

MicroRNAs (miRNAs) are non-coding, endogenous RNAs, which show a high level of conservation in the genomes of the majority of species. The dysregulation of miRNAs has been reported to be involved in the progression of OS and OS-derived cells through effects on the malignant phenotype of the cells or sensitivity to chemotherapy (4,5). miRNA (miR)-494 has been investigated in several types of tumor, including non-small cell lung cancer, liver cancer, cholangiocarcinoma, gastric cancer and pancreatic cancer (6-10). However, the modulatory effect of miR-494 differs in different types of tumor. For example, miR-494 can induce resistance of tumor necrosis factor-related apoptosis-inducing ligand and enhance G1/S transition leading to promotion of the malignant feather of liver cancer (11). By contrast, miR-494 exerts tumor-suppressive effects in ovarian cancer and epithelial ovarian cancer via inhibiting cell growth and promoting apoptosis (12,13). miR-494 has also been reported to induce the activation of drug resistance, which is mediated by the suppression of bone marrow stromal cells in acute myeloid leukemia cells (14). According to these findings, the pathophysiological mechanisms underlying the effects of miR-494 in tumors and other diseases are complex and numerous, requiring further investigations.

In the present study, deregulated miR-494 was identified in OS tissues and OS cells. miR-494 was found to function as a tumor suppressor in the development of OS by inhibiting proliferation and cell metastasis, and inducing cell cycle arrest in OS cells. Previous studies have demonstrated that cyclin-dependent kinase 6 (CDK6) is vital in the G1/S transition, and the inhibition of CDK6 can lead to cell cycle arrest (15). In accordance, the data obtained in the present study demonstrated that CDK6 is a potential target of miR-494.

An increase in the level of CDK6 was closely associated with the malignant phenotype of OS. These findings indicated that miR-494 exerted a tumor suppressive effect in OS, the function of which may be mediated by CDK6, providing a potential diagnostic and therapeutic target for the treatment of OS.

## Materials and methods

*Human OS tissues and cells*. A total of 18 patients (male, 10; female, 8; age ≤18 years, 13; age >18 years, 5; tumor stage I+II, 15; tumor stage III, 3) diagnosed with OS were recruited from the Second Affiliated Hospital, Chongqing Medical University (Chongqing, China). These patients were divided into two groups (metastasis, vs. no metastasis) according to radiological results. All patients provided written informed consent. The experimental protocols were approved by the Ethics Committee of the Second Affiliated Hospital, Chongqing Medical University. The OS tissues and the corresponding normal tissues (5 cm from the tumor margin) were obtained from resection and then immediately snap frozen in liquid nitrogen for storage at -80˚C.

The OS-derived human HOS, Saos2, U2OS and MG-63 cell lines, and the NHOst normal osteoblast cell line were purchased from Shanghai Cell Bank, Chinese Academy of Sciences (Shanghai, China). The cells were maintained in DMEM with 10% fetal bovine serum (FBS; Gibco; Thermo Fisher Scientific, Inc., Waltham, MA, USA) and incubated in a humidified atmosphere containing 5% $CO_2$ at 37˚C.

*RNA extraction and reverse transcription-quantitative polymerase chain reaction (RT-qPCR) analysis*. Total RNA was extracted from the tissues and cell lines using an RNeasy Plus Mini kit (Qiagen GmbH, Hilden, Germany) according to the manufacturer's instructions. Total RNA (2 $\mu$g) was purified and reverse transcribed into cDNA using a PrimeScript RT Reagent kit (Perfect Real-Time) from Takara Bio, Inc. (Otsu, Japan) according to the manufacturer's instructions. The qPCR analysis was performed on an ABI 7500 Fast Real-Time PCR system (Applied Biosystems; Thermo Fisher Scientific, Inc.) with a SYBR Premix Ex Taq™ II kit (Takara Bio, Inc.). The reaction mix contained 2 $\mu$l cDNA, 10 $\mu$l 2X Premix Ex Taq (Probe qPCR), 0.4 $\mu$l forward/reverse primers, 0.8 $\mu$l Probe, 0.2 $\mu$l ROX Reference Dye II and 6.2 $\mu$l $ddH_2O$ in a total volume of 20 $\mu$l. The sequences of the primers were as follows: miR-494 forward, 5'-TGACCTGAAACATACACG GGA-3', and reverse, 5'-TATCGTTGTACTCCACTCCTT GAC-3'; U6 forward, 5'-AAAGACCTGTACGCCAACAC-3' and reverse, 5'-GTCATACTCCTGCTTGCTGAT-3'. The PCR cycling conditions were as follows: 95˚C for 3 min, followed by 40 cycles of 95˚C for 30 sec, 62˚C for 30 sec and 72˚C for 30 sec. The results were calculated using the $2^{-\Delta\Delta Cq}$ method (16) and normalized to the expression of U6.

*Bioinformatics*. PicTar (http://pictar.mdc-berlin.de/), TargetScan (http://www.targetscan.org) and miRBase (http://www.mirbase.org/) (17-19) were used to investigate the potential binding sites of miR494.

*Luciferase reporter gene assay*. The wild-type 3'-untranslated region (3'-UTR) of CDK6 containing the miR-494 binding site was cloned into the pGL3-control vector (Ambion; Thermo Fisher Scientific, Inc.) to construct the CDK6-3'-UTR-wild-type (WT). The CDK6 3'-UTR mutations containing mutant (mut) sequences were obtained using a QuikChange Lightning Site-Directed Mutagenesis kit (Agilent Technologies, Inc., Palo Alto, CA, USA). All plasmids were confirmed by sequencing. The miR-494 mimics were generated by Shanghai GenePharma Co., Ltd. (Shanghai, China) and the scramble sequence was purchased from Ambion; Thermo Fisher Scientific, Inc. Briefly, the MG-63 (~2-3x$10^6$) and U2OS cells (~2-3x$10^6$) were seeded into a 24-well plate 1 day prior to transfection, and then co-transfected with miR-494 mimics (sense, 5'UGAAACAUACACGGGAAACCUC3' and antisense, 5'GGUUUCCCGUGUAUGUUUCAUU3'; 100 nM) or scramble (sense, 5'UUCUCCGAACGUGUCACGUUU3' and antisense, 5'ACGUACACGUUCGGAGAAUU3'; 50 nM), in addition to the CDK6-3'-UTR-WT or CDK6-3'-UTR-mutusing Lipofectamine 2000 (Invitrogen; Thermo Fisher Scientific, Inc.). After 48 h, the luciferase activity was determined using a Dual-Luciferase reporter assay (Promega Corporation, Madison, WI, USA), which was normalized to the activity of *Renilla* luciferase.

*Cell proliferation assays*. In order to evaluate the effect of the overexpression of miR-494 on cell proliferation, MTT assay and colony formation assays were performed. Briefly, 1x$10^3$ cells (MG-63 and U2OS cells) were seeded in 96-well plates with four repeats and then transfected with the miR-494 mimics or scramble control. The cell viability was assessed 48 h following transfection using an MTT kit (Sigma-Aldrich; Merck KGaA, Darmstadt, Germany). The results were determined at an optical density of 570 nm on a Tecan Spectra Fluor microplate reader (Tecan Group, Ltd., Männedorf, Switzerland). For the colony formation assay, ~200 transfected cells (miR-494 mimics or Scramble) were seeded in a 6-well plate with four repeats and cultured in DMEM containing 10% FBS for 2 weeks at 37˚C. The medium was replaced every 3 days.The colonies were fixed with methanol, stained with 0.1% crystal violet (Sigma-Aldrich; Merck KGaA) and subsequently counted under a light microscope.

*Cell invasion and migration assay*. In order to investigate the effect of the overexpression of miR-494 on cell invasion and migration, the present study examined metastasis using an assay with BD Matrigel invasion chambers (BD Biosciences, San Jose, CA, USA). A total of 4x$10^4$ cells (MG-63 and U2OS cells) transfected with miR-494 mimics or scramble control were cultured in serum-free DMEM medium and subsequently placed into the upper chamber, which was Matrigel-coated for the cell invasion assay or Matrigel-free for the migration assay. Simultaneously, 10% FBS was added into the lower chambers to function as a chemoattractant. Following incubation for 48 h at 37˚C, the cells on the upper surface of the membranes were removed, and the cells on the lower surface were fixed and stained (0.1% crystal violet). Images of the cells were captured and the number of cells were counted under a microscope (IX71; Olympus, Tokyo, Japan) in five randomly selected fields (magnification, x200).

*Cell cycle analysis*. A total of 1x$10^4$ MG-63 and U2OS cells were first transfected with miR-494 mimics or scramble control.

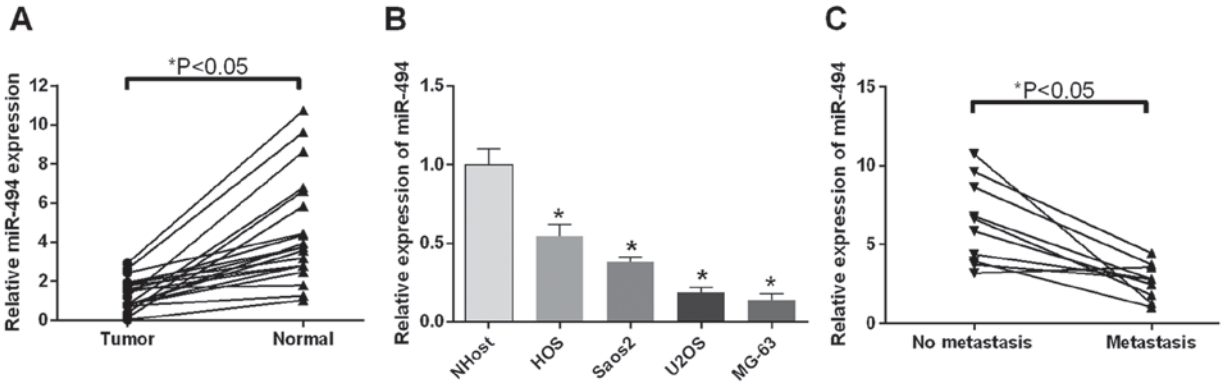


Figure 1. Relative expression of miR-494 in OS tissues and OS cell lines. (A) Expression levels of miR-494 in 18 patient tissue pairs were detected using RT-qPCR analysis. The expression of miR-494 was repressed in tumor tissues compared with normal tissues; (B) RT-qPCR results of the expression of miR-494 in HOS, Saos2, U2OS, MG-63 cells (OS cell lines) and NHOst cells. The expression of miR-494 was repressed in OS cells, compared with NHOst cells. (C) RT-qPCR results of the expression of miR-494 in the metastasis group and no metastasis group. The expression of miR-494 was repressed in the metastasis group, compared with that in the no metastasis group. *P<0.05. OS, osteosarcoma; RT-qPCR, reverse transcription-quantitative polymerase chain reaction; miR, microRNA.

After 48 h, the transfected cells were digested, collected and washed with PBS. Following washing twice with PBS, the cells were fixed with 70% ethanol at 4˚C overnight. Propidium iodide (PI) staining solution (50 $\mu$g/ml; 1 mg/ml of RNase A, 0.1% Triton X-100 in PBS) was added into the cell suspension. Finally the cells were examined on a BD FACSCalibur flow cytometer (BD Biosciences). The experiments were repeated three times.

*In vivo growth assay*. To examine the role of miR-494 *in vivo*, 20 female BALB/C-nu/nu mice (4-5 weeks old; weight, ~18-25 g) were used, which were purchased from the Animal Center of the Cancer Institute of Chinese Academy of Medical Science (Beijing, China). The study protocol was approved by the Ethics Committee of the Second Affiliated Hospital, Chongqing Medical University. The mice were maintained on a standard 12:12 h light-dark cycle with free access to food and water at 18-22˚C and with 50-60% humidity. The mice were randomly dived into two groups: the Lv-miR-494 group and the Lv-control group. A total of $2x10^6$ MG-63 cells transfected with miR-494 (Lv-miR-494 group) or the corresponding control (Lv-control) were subcutaneously injected into the flank region of the female nude mice. The mice were monitored every 3 days. After 5 weeks, the mice were sacrificed and the tumor tissues were measured on the basis of their width and length: (length x $width^2$)/2.

*Western blot analysis*. Following transfection, the cells were washed three times with PBS and lysed with radioimmunoprecipitation assay lysis buffer to obtain the total protein. Protein concentration was measured using a bicinchoninic acid protein assay kit (Pierce; Thermo Fisher Scientific, Inc.). Total proteins (50 $\mu$g) were separated by 10% SDS-PAGE and then transferred onto polyvinylidene fluoride membranes, as previously described (20). The membranes were incubated with blocking buffer (5% skimmed milk) for 1.5 h at room temperature and then incubated with the following primary antibodies: anti-CDK6 (1:500, ab79454; Abcam, Cambridge, MA, USA) and anti-GAPDH antibody (1:500; SAB4300645-100UG; Sigma-Aldrich, Merck KGaA) at 4˚C overnight. Following incubation with the primary antibody, blots were washed with TBS-0.1% Tween and subsequently incubated with horseradish peroxidase-conjugated goat anti-rabbit (1:2,000, ab6721) or rabbit anti-mouse IgG (1:2,000, ab6709) (both from Abcam) secondary antibodies at 37˚C for 2 h. Band intensity was quantified using Immobilon Western Chemiluminescent HRP Substrate (EMD Millipore, Billerica, MA, USA). Experiments were performed in triplicate.

*Statistical analysis*. Statistical analysis was performed using the SPSS 13.0 software package (SPSS, Inc., Chicago, IL, USA) using one-way analysis of variance followed by the Student-Newman-Keuls post hoc test. P≤0.05 was considered to indicate a statistically significant difference.

## Results

*miR-494 is downregulated in OS tissues and cells*. The present study used RT-qPCR analysis to examine the expression profiles of miR-494 in OS tumor tissues (metastatic, vs. non-metastatic), cell lines and corresponding controls. It was found that the expression levels of miR-494 in the 18 patients were significantly downregulated, compared with those in the normal tissues (P<0.05; Fig. 1A). In accordance, the expression levels of miR-494 in the HOS, Saos2, U2OS, MG-63 OS cells were significantly downregulated, compared with that in the NHOst cells (P<0.05; Fig. 1B). The association between cell metastasis and the expression of miR-494 was also investigated. The results suggested that the expression of miR-494 was decreased in the metastatic group, compared with the non-metastatic group (P<0.05; Fig. 1C). These findings indicated that the expression of miR-494, which was downregulated in OS tissues and cells, was closely linked to tumor metastasis.

*Restoration of the expression of miR-494 inhibits proliferation in vitro and in vivo*. As primary cells from human OS tissues are difficult to culture, MG-63 and U2OS cells were selected for the subsequent experiments, due to their routine maintenance in cell culture and ubiquitous

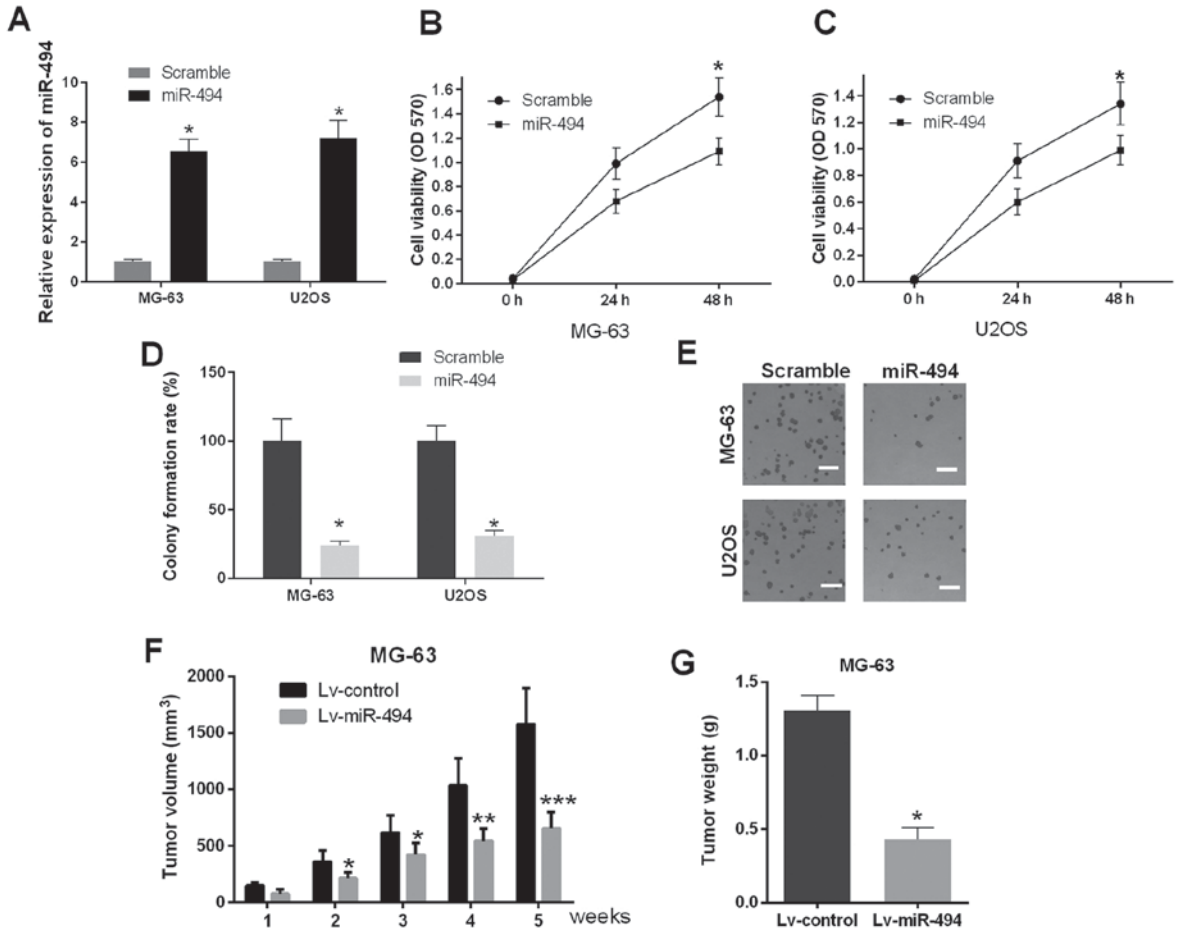


Figure 2. miR-494 suppresses cell proliferation *in vitro* and *in vivo*. (A) Confirmation of the expression of miR-494 in MG-63 and U2OS cells transfected with miR-494 mimics and scramble. Viability of MG-63 and U2OS cells were detected using MTT assay. Overexpression of miR-494 in (B) MG-63 cells and (C) U2OS cells significantly inhibited cell viability. (D) Colony formation assay to investigate the effect of miR-494 on cell growth of MG-63 and U2OS cells. Overexpression of miR-494 in MG-63 and U2OS cells result in inhibited cell growth. (E) Representative images of MG-63 and U2OS cells under a microscope (magnification, x200). (F) Tumor volumes were measured 1, 2, 3, 4 and 5 weeks following injection of Lv-miR-494 and Lv-control. The volumes of tumors injected with Lv-miR-494 were significantly decreased compared with those injected with Lv-control. (G) Overexpression of miR-494 significantly inhibited tumor weight *in vivo* 5 weeks following injection. $^{*}$P<0.05, $^{**}$P<0.01 and $^{***}$P<0.001. miR, microRNA; OD, optical density.

use in investigations of OS (21,22). In addition, MG-63 and U2OS cells are OS-derived human cell lines with differing proliferation potential, providing the opportunity to examine different types of the disease: MG-63 cells exhibit a low level of proliferation, whereas U2OS cells exhibit more malignant proliferation potential (23). In the present study, miR-494 mimics were transfected into MG-63 and U2OS cells, MTT and cell colony formation assays were used to investigate the effect of the promotion of miR-494 on cell proliferation *in vitro* (48 h post-transfection). The results of the RT-qPCR analysis showed that the expression of miR-494 was significantly elevated in the cells transfected with miR-494 mimics (P<0.05; Fig. 2A). The results of the MTT assay suggested that the ectopic expression of miR-494 resulted in cell growth inhibition, compared with the scramble control group in MG-63 and U2OS cells (P<0.05; Fig. 2B and C). The results of the cell colony formation assays confirmed that the cells transfected with miR-494 mimics exhibited decreased cell numbers (P<0.05; Fig. 2D and E), which was in accordance with the MTT assays. To further determine the underlying regulatory effects of miR-494 *in vivo*, female nude mice were subcutaneously injected with miR-494 lentivirus (Lv-miR-494) and Lv-control, respectively. The data indicated that injection of miR-494 significantly suppressed tumor volume and weight, compared with those in the Lv-control group, and this effect was time-dependent. (P<0.05, P<0.01 and P<0.001; Fig. 2F and G). Taken together, these findings demonstrated that the ectopic expression of miR-494 caused marked cell growth inhibition *in vitro* and *in vivo*.

*Overexpression of miR-494 inhibits cell metastasis and induces cell cycle arrest in OS cells*. As the overexpression of miR-494 inhibited proliferation *in vitro* and *in vivo*, the present study performed invasion and migration assays to evaluate the effect of the restoration of miR-494 on cell metastasis. As shown in Fig. 3A and B, the numbers of MG-63 and U2OS cells in the miR-494 group were decreased, compared with the number in the scramble group (P<0.05), which indicated that cell invasion in the miR-494 group was repressed relative to the control. In addition, the numbers of migrated MG-63 and U2OS cells in the miR-494 group were decreased, compared with the number in the scramble group, which was consistent with the results of the cell invasion assay (P<0.05; Fig. 3C and D). The effect of

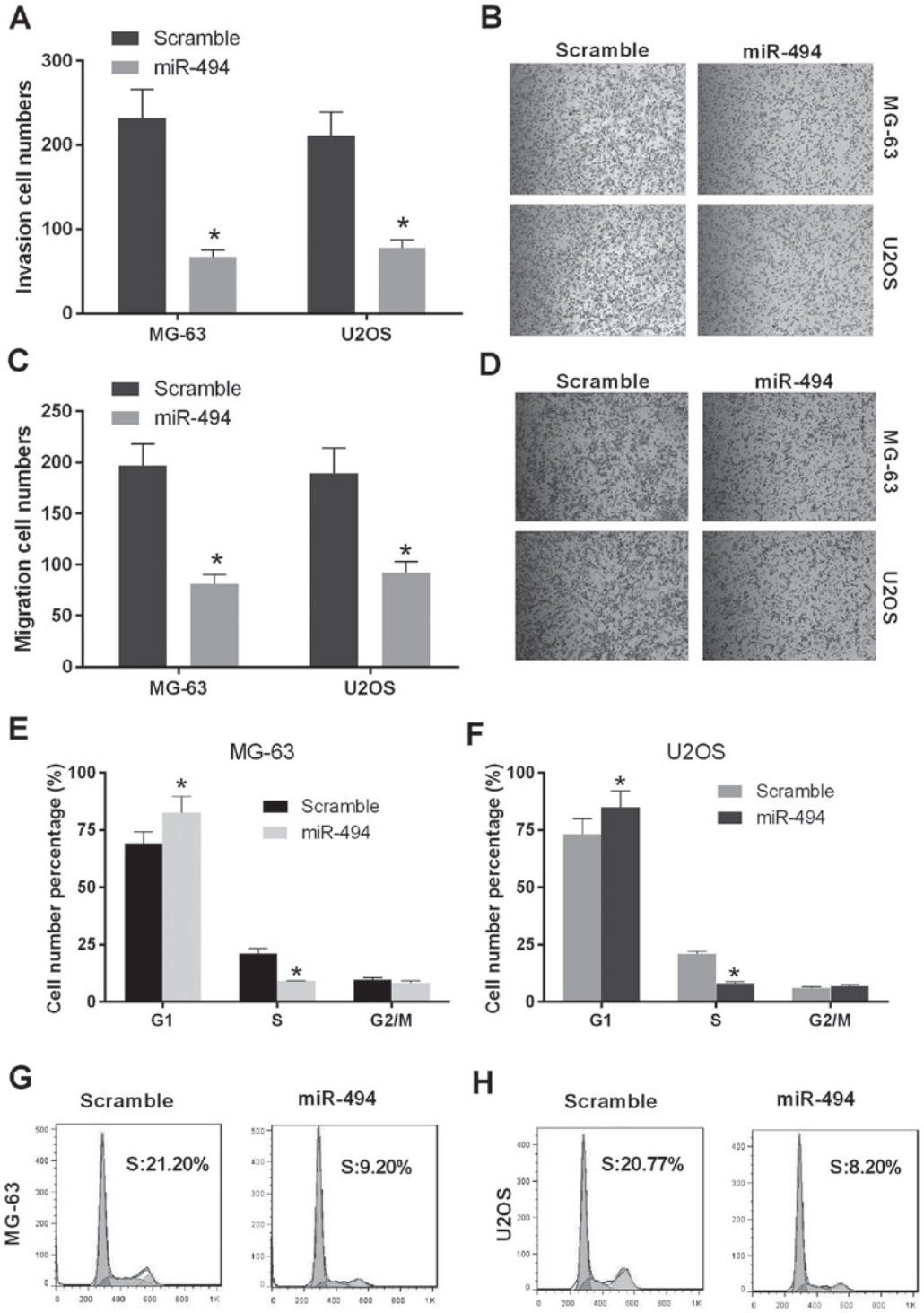


Figure 3. miR-494 suppresses cell metastasis *in vitro*. (A) The number of cells transfected with miR-494 was decreased compared with cells transfected with scramble in the MG-63 and U2OS cells. The restoration of miR-494 significantly repressed cell invasion of MG-63 and U2OS cells. (B) Representative images of MG-63 and U2OS cells under a microscope (magnification, x200) in the cell invasion assay. (C) Following transfection with miR-494, a decrease in the number of migrated cells was observed, compared with the cells transfected with scramble in the MG-63 and U2OS cells. The restoration of miR-494 significantly repressed the migration of the MG-63 and U2OS cells. (D) Representative images of MG-63 and U2OS cells under a microscope in the cell migration assay. Flow cytometric analysis was used to detect cell cycle distribution in the MG-63 and U2OS cells following transfection with miR-494 or scramble. Overexpression of miR-494 resulted in a promotion of the G1-phase and decrease of the S-phase in the (E) MG-63 and (F) U2OS cells. Flow cytometric analysis of the (G) MG-63 and (H) U2OS cells transfected with miR-494 or scramble. *P<0.05. miR, microRNA.

miR-494 on cell cycle progression was then investigated in MG-63 and U2OS cells. The results showed that the ectopic expression of miR-494 in the MG-63 cells and U2OS cells significantly increased in the number of G1-phase cells and reduced the number of S-phase cells (P<0.05; Fig. 3E-H). Taken together, these findings suggested that miR-494 inhibited cell metastasis and induced cell cycle arrest of the OS cells.

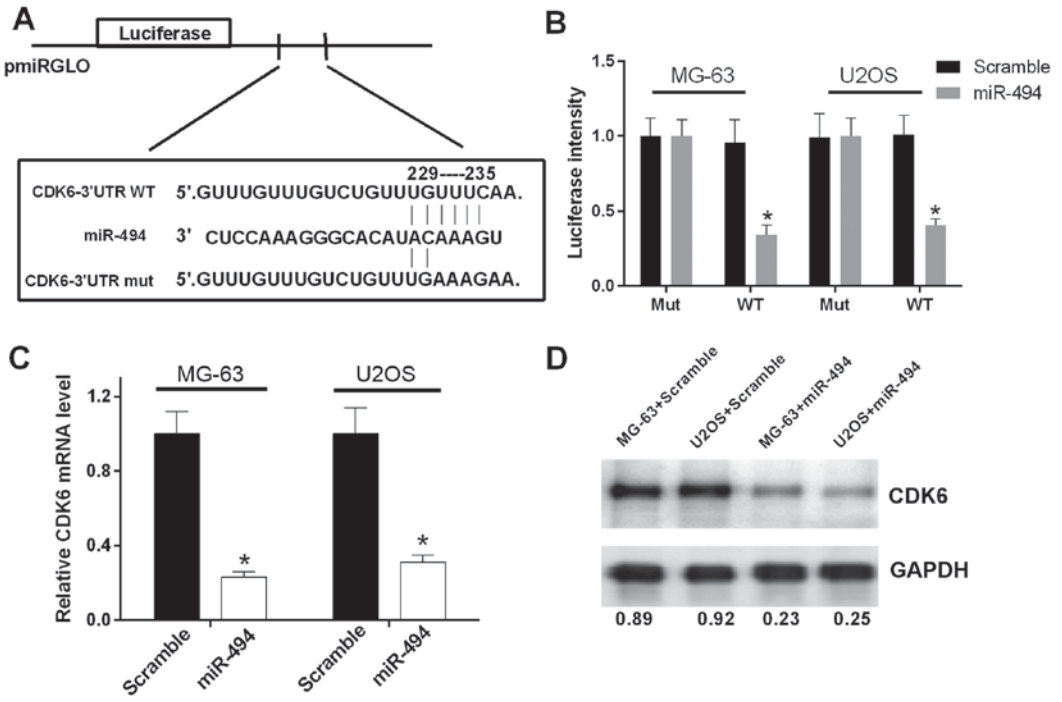


Figure 4. miR-494 directly targets CDK6 and inversely regulates its expression. (A) Bioinformatics analysis showed that miR-494 potentially targeted CDK6. (B) Luciferase assays were used to investigate the potential target of miR-494, which revealed CDK6 as a direct target of miR-494. Expression of CDK6 was detected using (C) reverse transcription-quantitative polymerase chain reaction and (D) western blot analysis in the MG-63 and U2OS transfected with miR-494 or scramble. miR-494 negatively regulated the expression of CDK6. *P<0.05. miR, microRNA; CDK6, cyclin-dependent kinase 6.3'UTR, 3'untranslated region; WT, wild-type; mut, mutant.

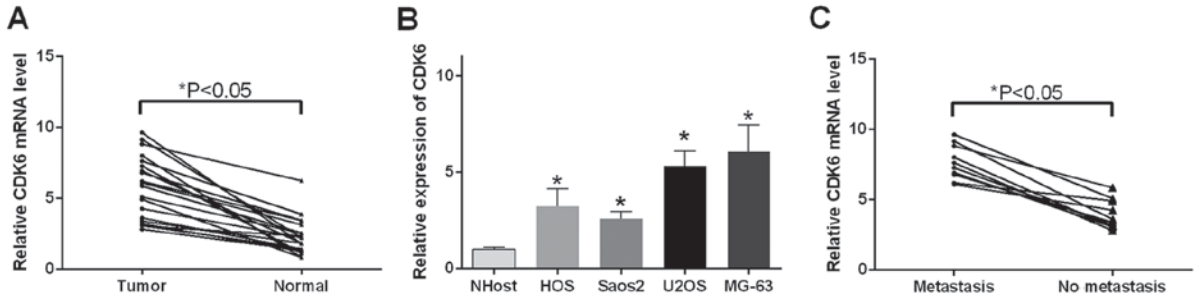


Figure 5. Relative expression of CDK6 in OS tissues and different OS cell lines. (A) Expression levels of CDK6 were significantly promoted in tumor tissues, compared with normal tissues. (B) Results of reverse transcription-quantitative polymerase chain reaction analysis of the expression of CDK6 in HOS, Saos2, U2OS and MG-63 cells (OS cell lines), and NHOst cells. (C) mRNA expression of CDK6 was elevated in the group with metastasis, compared with the group with no metastasis. *P<0.05. OS, osteosarcoma; miR, microRNA; CDK6, cyclin-dependent kinase 6.

*miR-494 directly targets CDK6 and suppresses its expression*. As miR-494 has been reported to be involved in tumor progression via base-pairing to the 3'-UTR of its target genes, bioinformatics analysis was performed using PicTar, TargetScan and miRBase to predict the potential target of miR-494. The results revealed an miR-494 binding site in the CDK6 3'-UTR (Fig. 4A). In order to validate whether the 3'-UTR of CDK6 is a functional target of miR-494, a luciferase reporter assay was performed. The results showed that the promoted expression of miR-494 suppressed the luciferase activity of the CDK6 3'-UTR-WT construct, but not the CDK6 3'-UTR-mut construct in OS cells (P<0.05; Fig. 4B). In addition, RT-qPCR and western blot analyses were performed to evaluate the effect of promoted miR-494 on the expression of CDK6. The elevated expression of miR-494 resulted in reductions in the mRNA and protein expression of CDK6 in the MG-63 and U2OS cells (P<0.05; Fig. 4C and D). These data indicated that miR-494 directly targeted CDK6 and negatively regulated the expression of CDK6.

*CDK6 is upregulated in OS tissues and cells*. As it was found that miR-494 directly targeted CDK6 and regulated the expression of CDK6, the present study investigated the expression pattern of CDK6 in the OS tissue and cells. The results of the RT-qPCR analysis indicated that CDK6 mRNA was upregulated in the 18 OS tissue samples (P<0.05; Fig. 5A) and OS cells (P<0.05; Fig. 5B), compared with the corresponding controls, respectively. In addition, the expression of CDK6 was examined in tissues with differing features of metastasis. It was observed that the tissues in the metastasis group exhibited increased levels of CDK6, compared with those in the no metastasis group (P<0.05; Fig. 5C).

## Discussion

An increasing number of studies have focused on the pathophysiological and physiological mechanisms of miRNAs in tumor progression. miRNAs can either positively or negatively affect the development of tumors depending on their specific downstream target genes by base-pairing with their 3'-UTR. For example, miR-24 can induce chemotherapy resistance and hypoxic advantage in breast cancer through the downregulation of factor inhibiting HIF-1 (24). miR-497 is significantly correlated with temozolomide-resistance in glioma cells by regulating the insulin-like growth factor 1 receptor/insulin receptor substrate 1 pathway (25). miR-93 is known to affect metastatic spread in breast carcinoma through the regulation of protein kinase WNK1 (26). miR-152 has been demonstrated to target phosphatase and tensin homolog in nasopharyngeal carcinoma cells by promoting cell migration and inhibiting apoptosis (27). The abnormal expression of miRNAs has also been shown to be involved in the pathogenesis and progression of OS. For example, miR-150 has been reported as a tumor suppressor in the development of OS, by targeting insulin-like growth factor 2 mRNA-binding protein 1 (28). miR-92a functions as a driver of tumor progression, which can promote tumor growth in OS by suppressing F-box and WD repeat-containing protein 7 (29). The present study aimed to investigate the potential role of miR-494 in the development of OS.

The function ofmiR-494 as a tumor suppressor in OS was identified in the present study, which induced cell growth inhibition through the regulation of CDK6. The malignant phenotype of tumors is closely linked to the irregular proliferation of cells. Several studies have focused on the diagnostic and therapeutic targets of cytological features. The results of these investigations provide evidence that the ectopic expression of miR-494-3p in PC-3 and DU145 cells inhibits proliferation and metastasis, and sell apoptosis (30). In addition, miR-494 exhibits a suppressive function in gastric cancer by inhibiting cell invasion and proliferation (31). In accordance, the findings of the present study indicated that the overexpression of miR-494 resulted in cell growth inhibition and cell cycle arrest at the G1/S phase in MG-63 and U2OS cells. In addition, the data obtained from animal experiments indicated that the injection of miR-494 significantly suppressed tumor volume and weight *in vivo*. In separate experiments, patients were divided into two groups according to metastasis, and radiological results were examined to determine the correlation between the expression of miR-494 and cell metastasis. The data indicated that the group exhibiting metastasis exhibited inhibited expression of miR-494, compared with the group without metastasis. Taken together, these results indicated the decreased expression of miR-494 was involved in the development of OS.

The present study also performed bioinformatics analysis and luciferase reporter gene assay to examine the potential targets of miR-494. The results showed that CDK6 was a direct target of miR-494. CDK6 is vital in cell cycle progression, and inhibition of CDK6 leads to uncontrolled tumor cell proliferation, which is a major hallmark of cancer (32). The function of CDK6 in cell progression has been found in several types of cancer, including glioblastoma, myxofibrosarcoma and lymphoid malignancies (33,34). In accordance with these findings, the results of the present study suggested that CDK6 was significantly upregulated in OS tissues and cells, compared with corresponding controls. The expression of CDK6 was further investigated in tissues of differing malignant phenotypes (metastasis and no metastasis) and found that the metastatic tumors exhibited elevated expression of CDK6. Taken together, these data indicated that CDK6 promoted the progression of OS. miR-494 was shown to exert a tumor suppressive function in the development of OS, and CDK6, which functions as an oncogene in OS, is a direct target of miR-494. The role of miR-494 in OS tissues and cells may be mediated by CDK6. However, the exact effect of CDK6 dysregulation was not investigated in the present study.

In conclusion, the results of the present study suggested that the miR-494-induced inhibited expression of CDK6 in OS may be a useful epigenetic therapeutic approach, although further experiments are required to determine this.

## Acknowledgements

This work was supported by grants from the Natural Science Foundation of China (NSFC 81672230 and 81501867) and the Key Project of Science and Technology Commission of Chongqing (CTSC 2013jcyjA10090).

## References

1. Luetke A, Meyers PA, Lewis I and Juergens H: Osteosarcoma treatment-where do we stand? A state of the art review. Cancer Treat Rev 40: 523-532, 2014.
2. Benjamin RS: Osteosarcoma: Better treatment through better trial design. Lancet Oncol 16: 12-13, 2015.
3. Xiong Y, Wu S, Du Q, Wang A and Wang Z: Integrated analysis of gene expression and genomic aberration data in osteosarcoma (OS). Cancer Gene Ther 22: 524-529, 2015.
4. Lulla RR, Costa FF, Bischof JM, Chou PM, de F Bonaldo M, Vanin EF and Soares MB: Identification of differentially expressed microrna in osteosarcoma. Sarcoma 2011: 732690, 2011.
5. Marina N, Gebhardt M, Teot L and Gorlick R: Biology and therapeutic advances for pediatric osteosarcoma. Oncologist 9: 422-441, 2004.
6. Romano F, Garancini M, Uggeri F, Degrate L, Nespoli L, Gianotti L, Nespoli A and Uggeri F: Surgical treatment of liver metastases of gastric cancer: State of the art. World J Surg Oncol 10: 157, 2012.
7. Olaru AV, Ghiaur G, Yamanaka S, Luvsanjav D, An F, Popescu I, Alexandrescu S, Allen S, Pawlik TM, Torbenson M, *et al*: MicroRNA down-regulated in human cholangiocarcinoma control cell cycle through multiple targets involved in the G1/S checkpoint. Hepatology 54: 2089-2098, 2011.
8. Hong KJ, Wu DC, Cheng KH, Chen LT and Hung WC: RECK inhibits stemness gene expression and tumorigenicity of gastric cancer cells by suppressing ADAM-mediated Notch1 activation. J Cell Physiol 229: 191-201, 2014.
9. Ma YB, Li GX, Hu JX, Liu X and Shi BM: Correlation of miR-494 expression with tumor progression and patient survival in pancreatic cancer. Genet Mol Res 14: 18153-18159, 2015.
10. Tian C, Zheng G, Zhuang H, Li X, Hu D, Zhu L, Wang T, You MJ and Zhang Y: MicroRNA-494 activation suppresses bone marrow stromal cell-mediated drug resistance in acute myeloid leukemia cells. J Cell Physiol 232: 1387-1395, 2017.
11. Lim L, Balakrishnan A, Huskey N, Jones KD, Jodari M, Ng R, Song G, Riordan J, Anderton B, Cheung ST, *et al*: MicroRNA-494 within an oncogenic microRNA megacluster regulates G1/S transition in liver tumorigenesis through suppression of mutated in colorectal cancer. Hepatology 59: 202-215, 2014.
12. Zhao X, Zhou Y, Chen YU and Yu F: miR-494 inhibits ovarian cancer cell proliferation and promotes apoptosis by targeting FGFR2. OncolLett 11: 4245-4251, 2016.

13. Yuan J, Wang K and Xi M: miR-494 inhibits epithelial ovarian cancer growth by targeting c-Myc. Med Sci Monit 22: 617-624, 2016.
14. Tian C, Zheng G, Zhuang H, Li X, Hu D, Zhu L, Wang T, You MJ and Zhang Y: MicroRNA-494 activation suppresses bone marrow stromal cell-mediated drug resistance inacute myeloid leukemia cells. J Cell Physiol 232: 1387-1395, 2017.
15. Rader J, Russell MR, Hart LS, Nakazawa MS, Belcastro LT, Martinez D, Li Y, Carpenter EL, Attiyeh EF, Diskin SJ, *et al*: Dual CDK4/CDK6 inhibition induces cell-cycle arrest and senescence in neuroblastoma. Clin Cancer Res 19: 6173-6182, 2013.
16. Livak KJ and Schmittgen TD: Analysis of relative gene expression data using real-time quantitative PCR and the 2(-Delta Delta C(T)) method. Methods 25: 402-408, 2001
17. Krek A, Grün D, Poy MN, Wolf R, Rosenberg L, Epstein EJ, MacMenamin P, da Piedade I, Gunsalus KC, Stoffel M and Rajewsky N: Combinatorial microRNA target predictions. Nat Genet 37: 495-500, 2005.
18. Agarwal V, Bell GW, Nam JW and Bartel DP: Predicting effective microRNA target sites in mammalian mRNAs. Elife: 4, 2015.
19. Griffiths-Jones S, Saini HK, van Dongen S and Enright AJ: miRBase: Tools for microRNA genomics. Nucleic Acids Res 36 (Database issue): D154-D158, 2008.
20. Liu S and Feng P: miR-203 determines poor outcome and suppresses tumor growth by targeting tbk1 in osteosarcoma. Cell Physiol Biochem 37:1956-1966, 2015.
21. Vanas V, Haigl B, Stockhammer V and Sutterlüty-Fall H: MicroRNA-21 increases proliferation and cisplatin sensitivity of osteosarcoma-derived cells. PLoS One 11: e0161023, 2016.
22. Yao J, Qin L, Miao S, Wang X and Wu X: Overexpression of miR-506 suppresses proliferation and promotes apoptosis of osteosarcoma cells by targeting astrocyte elevated gene-1. Oncol Lett 12: 1840-1848, 2016.
23. Li Y, Liu J, Liu ZZ and Wei WB: MicroRNA-145 inhibits tumour growth and metastasis in osteosarcoma by targeting cyclin-dependent kinase, CDK6. Eur Rev Med Pharmacol Sci 20: 5117-5125, 2016.
24. Roscigno G, Puoti I, Giordano I, Donnarumma E, Russo V, Affinito A, Adamo A, Quintavalle C, Todaro M, Vivanco MD and Condorelli G: miR-24 induces chemotherapy resistance and hypoxic advantage in breast cancer. Oncotarget 8: 19507-19521, 2017.
25. Zhu D, Tu M, Zeng B, Cai L, Zheng W, Su Z and Yu Z: Up-regulation of miR-497 confers resistance to temozolomide in human glioma cells by targeting mTOR/Bcl-2. Cancer Med 6: 452-462, 2017.
26. Shyamasundar S, Lim JP and Bay BH: miR-93 inhibits the invasive potential of triple-negative breast cancer cells *in vitro* via protein kinase WNK1. Int J Oncol 49: 2629-2636, 2016.
27. Huang S, Li X and Zhu H: MicroRNA-152 targets phosphatase and tensin homolog to inhibit apoptosis and promote cell migration of nasopharyngeal carcinoma cells. Med Sci Monit 22: 4330-4337, 2016.
28. Qu Y, Pan S, Kang M, Dong R and Zhao J: MicroRNA-150 functions as a tumor suppressor in osteosarcomaby targeting IGF2BP1. Tumour Biol 37: 5275-5284, 2016.
29. Jiang X, Li X, Wu F, Gao H, Wang G, Zheng H, Wang H, Li J and Chen C: Overexpression of miR-92a promotes the tumor growth of osteosarcoma by suppressing F-box and WD repeat-containing protein 7. Gene 606: 10-16. 2017.
30. Shen PF, Chen XQ, Liao YC, Chen N, Zhou Q, Wei Q, Li X, Wang J and Zeng H: MicroRNA-494-3p targets CXCR4 to suppress the proliferation, invasion and migration of prostate cancer. Prostate 74: 756-767, 2014.
31. Zhao XQ, Liang TJ and Fu JW: miR-494 inhibits invasion and proliferation of gastric cancer by targeting IGF-1R. Eur Rev Med Pharmacol Sci 20: 3818-3824, 2016.
32. Handschick K, Beuerlein K, Jurida L, Bartkuhn M, Müller H, Soelch J, Weber A, Dittrich-Breiholz O, Schneider H, Scharfe M, *et al*: Cyclin-dependent kinase 6 is a chromatin-bound cofactor for NF-κB-dependent gene expression. Mol Cell 53: 193-208, 2014.
33. Wiedemeyer WR, Dunn IF, Quayle SN, Zhang J, Chheda MG, Dunn GP, Zhuang L, Rosenbluh J, Chen S, Xiao Y, *et al*: Pattern of retinoblastoma pathway inactivation dictates response to CDK4/6 inhibition in GBM. Proc Natl Acad Sci USA 107: 11501-11506, 2010.
34. Tsai JW, Li CF, Kao YC, Wang JW, Fang FM, Wang YH, Wu WR, Wu LC, Hsing CH, Li SH, *et al*: Recurrent amplification at 7q21.2 Targets CDK6 gene in primary myxofibrosarcomas and identifies CDK6 overexpression as an independent adverse prognosticator. Ann Surg Oncol 19: 2716-2725, 2012.